Research
A SCIENCE PARTNER JOURNAL

RESEARCH ARTICLE

Chromones as Photocatalyzed HAT Reagent and Michael Acceptor for Direct C–H Alkylation of 2-Substituted 4-Chromanones

Ya Xiao[1†], Junrong Zhang[1†], Wujun Jian[1], Ya Zhou[1], Xiang Zhou[1*], W. M. W. W. Kandegama[2], and Song Yang[1*]

[1]State Key Laboratory of Green Pesticides, Key Laboratory of Green Pesticide and Agricultural Bioengineering, Ministry of Education, Center for R&D of Fine Chemicals of Guizhou University, Guiyang 550025, China.
[2]Department of Horticulture and Landscape Gardening, Faculty of Agriculture and Plantation Management, Wayamba University of Sri Lanka, Makandura, Gonawila, Sri Lanka.

*Address correspondence to: zhoux1534@163.com (X.Z.); jhzx.msm@gmail.com (S.Y.)
†These authors contributed equally to this work.

Citation: Xiao Y, Zhang J, Jian W, Zhou Y, Zhou X, Kandegama WMWW, Yang S. Chromones as Photocatalyzed HAT Reagent and Michael Acceptor for Direct C–H Alkylation of 2-Substituted 4-Chromanones. *Research* 2026;9:Article 1250. https://doi.org/10.34133/research.1250

Submitted 7 January 2026
Revised 20 March 2026
Accepted 23 March 2026
Published 11 May 2026

Copyright © 2026 Ya Xiao et al. Exclusive licensee Science and Technology Review Publishing House. No claim to original U.S. Government Works. Distributed under a Creative Commons Attribution License (CC BY 4.0).

4-Chromanone is a biologically important heterocyclic scaffold found in natural products and pharmaceuticals. Traditional syntheses of 2-substituted 4-chromanones often rely on high-temperature peroxide initiation, transition-metal catalysis, or complex photocatalytic systems, limiting functional-group tolerance and sustainability. Herein, we report a Giese-type strategy for direct C–H functionalization of chromone derivatives, where chromones act as both substrates and hydrogen atom transfer (HAT) reagents to active inert C(sp^3)–H bonds and P–H bonds under mild, metal-free conditions. Upon light irradiation, chromones form triplet states that mediate HAT for diverse substrates, including ethers, esters, alcohols, alkanes, sulfides, and arylphosphines. The resulting radicals are captured by ground-state chromones, efficiently affording 2-substituted 4-chromanones. Mechanistic studies and density functional theory calculations support the radical-mediated pathway, and the method avoids the use of metal catalysts, external redox mediators, or photocatalysts, highlighting its scalability and sustainable potential.

Introduction

4-Chromanone constitutes an important oxygen-containing heterocyclic scaffold, whose derivatives exhibit diverse biological activities and are widely found in numerous biologically active molecules [1–4]. In particular, 2-substituted 4-chromanone derivatives display a broad range of bioactivities, including antibacterial [5,6], anti-inflammatory [7], antitumor [8], and antiproliferative effects against breast and lung carcinoma cell lines [9] (Fig. 1A). The broad biological activities of these compounds have drawn attention. Researchers are focusing on developing simple and efficient methods to synthesize 2-substituted 4-chromanones. Chromones belong to the class of α,β-unsaturated carbonyl compounds. In Giese-type reactions, they act as effective Michael acceptors to construct 2-substituted 4-chromanones. Traditional Giese additions using chromone substrates generally require either high-temperature initiation with di-*tert*-butyl peroxide [10–13], reactions involving transition metals such as zinc [14,15] and iron [16] (Fig. 1B).

In comparison, photocatalytic strategies offer a more sustainable alternative by employing light energy to drive chemical transformations under mild conditions. Through the rational design of photocatalysts and their active sites [17,18], diverse photocatalytic pathways have been developed [19,20]. Previous studies have reported the synthesis of 4-chromanone derivatives using various photocatalytic strategies [21–23], among which the combination of photocatalysis with hydrogen atom transfer (HAT) has emerged as an efficient approach. Photocatalytic HAT has been employed to directly construct a variety of carbon–carbon and carbon–heteroatom bonds [24–29], particularly enabling functionalization of inert C(sp^3)–H bonds under mild conditions [30–35]. Representative examples include $CuCl_2$-catalyzed synthesis of 2-substituted 4-chromenones via a photoinduced ligand-to-metal charge transfer (LMCT) pathway [36]. $Ru(bpy_3)_2(PF_6)_2$-catalyzed doubly decarboxylative Giese addition reported by Moczulski et al. [37], as well as light-driven C2-alkylation of chromones using decatungstate (TBADT) and zwitterionic acridinium-based HAT reagents developed by Entgelmeier et al. [38] and Qiao et al. [39], respectively (Fig. 1B). Additional photocatalytic HAT mediators include eosin Y [40,41] and metal complexes like $CuCl_2$ [42] and $FeCl_3$ [43,44]. Moreover, heteroatom-centered radicals derived from sulfur or nitrogen compounds [45–49] have been employed to promote radical additions to unsaturated systems. Despite these advances, current photocatalytic HAT systems are often limited by short excited-state lifetimes and inadequate site selectivity [50–53]. Reduced reaction efficiency caused by competing single-electron or energy-transfer processes remains another challenge [54,55]. Sulfur- and nitrogen-centered HAT reagents often rely on precious photocatalysts, increasing cost and

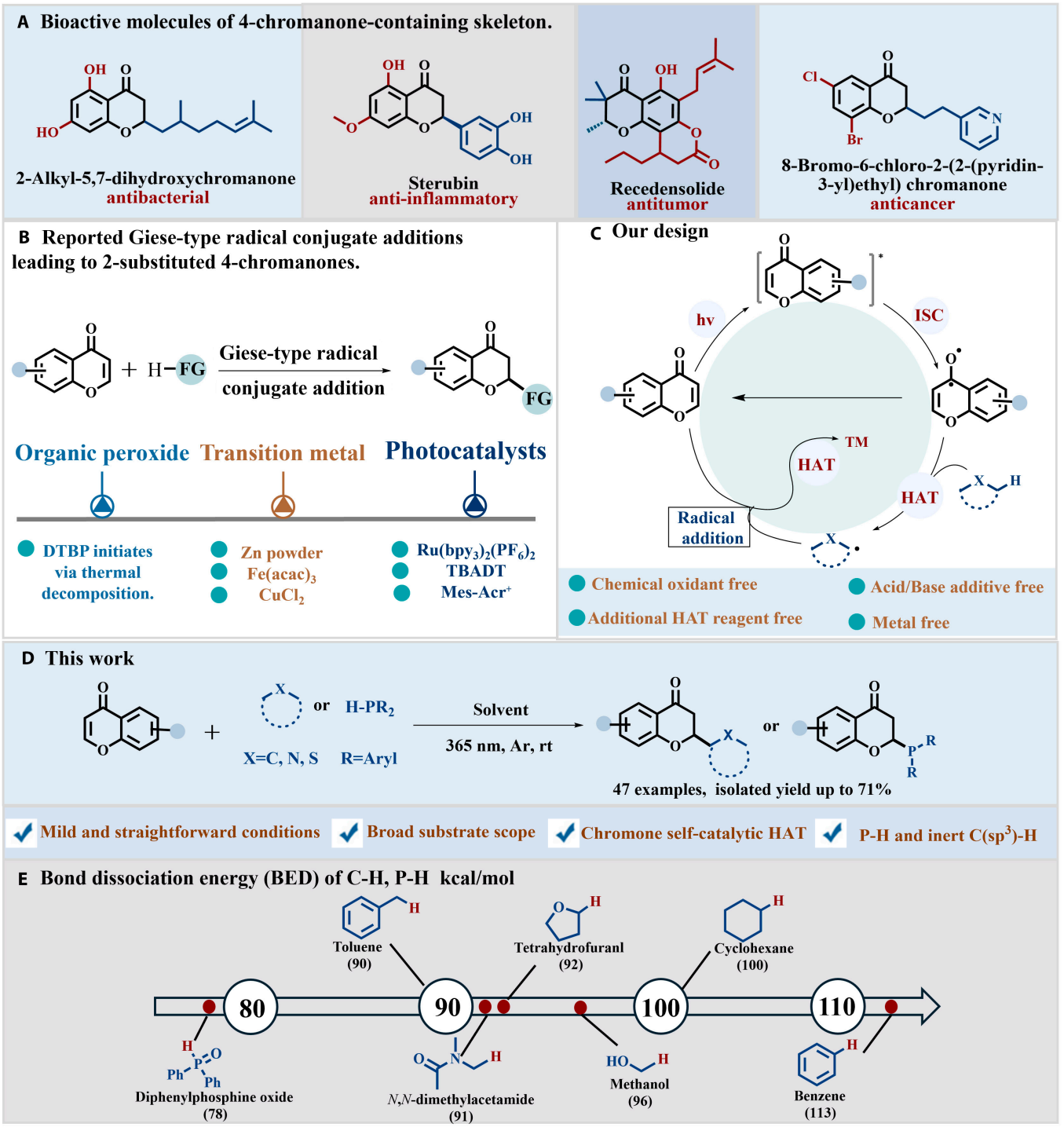


Fig. 1. (A) Bioactive molecules of 4-chromanone-containing skeleton. (B) Reported Giese-type radical conjugate additions leading to 2-substituted 4-chromanones. (C) Catalytic cycle of chromone serving as both HAT reagent and substrate. (D) This work. (E) BED of C–H, P–H kcal/mol.

reducing sustainability. These factors limit the broader application of photocatalytic HAT. Developing efficient, low-cost, metal-free organic HAT reagents is a promising direction.

Aromatic carbonyl compounds have attracted attention as photosensitizers and as HAT mediators because of their favorable photophysical properties [56,57]. Since the seminal works reporte by Norrish and Bamford in 1937 [58], the photoexcitation behavior of carbonyl compounds has been widely applied in synthetic transformations [59–61]. Upon light absorption, these compounds can undergo intersystem crossing to triplet excited states with diradical character [62], which allows hydrogen atom abstraction from a variety of substrates [63–69] and enables carbonyl-driven self-coupling without the need for external photocatalysts [70,71]. Using aromatic carbonyl compounds as both substrates and HAT mediators in Giese-type reactions remains relatively unexplored.

Herein, we designed photoexcited chromones as intrinsic HAT reagent, activating both P–H bonds and C–H bonds,

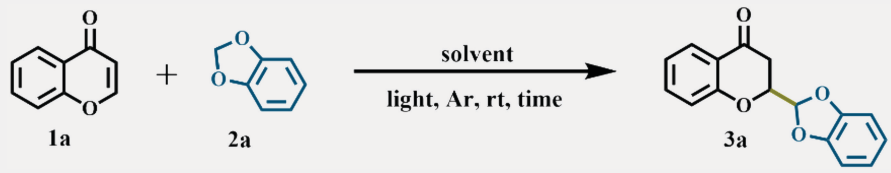
thereby enabling Giese-type addition reactions between ground-state chromones and substrates such as alkanes, ethers, esters, and arylphosphines (Fig. 1C and D). Compared with previous studies that rely on unstable peroxides, harsh reaction conditions, limited functional group compatibility, excessive involvement of metal reagents, and complex, costly photocatalytic systems, all of which are unfavorable for the development of green chemistry, this work utilizes chromones as Michael acceptors to construct 2-substituted 4-chromanones via Giese-type addition. This reaction system avoids the use of metal catalysts, unstable peroxides, external photocatalysts, redox reagents, or additional HAT mediators; can be performed under mild conditions; and demonstrates a chromone-mediated self-sustained HAT reaction mode, broad substrate applicability, and good alignment with green chemistry principles.

Results and Discussion

Optimization of the reaction conditions

To assess the feasibility of chromones as dual-functional substrates and intrinsic HAT mediators in Giese-type additions, chromone (**1a**) and benzodioxole (**2a**) were selected as model substrates for reaction condition optimization (Table 1). Initial screening of irradiation wavelengths (Table S1) demonstrated that irradiation with a 9-W 365-nm light-emitting diode (LED) light source for 12 h afforded the target product **3a** in 59% yield (Table 1, entry 1). Chromone compounds require light of sufficient energy to excite them to the triplet state necessary for the reaction, and irradiation at 365 nm efficiently generates this triplet state, thereby facilitating the HAT process. Subsequent solvent screening (Table S2) identified the moderate polarity solvent dichloroethane (DCE) as optimal, which also gave **3a** in 59% yield (Table 1, entry 1). Through comparison of the fluorescence intensities of excited-state chromones in different solvents, it was found that solvents with either excessively high or low polarity are unfavorable for stabilizing the excited state, whereas solvents with moderate polarity, such as DCE, effectively stabilize the excited state (Fig. S1). This observation is consistent with the experimental results. Thus, solvent polarity can affect the excited-state lifetime of chromones, which in turn influences HAT efficiency [72]. Further optimization of the loading of **2a** revealed that increasing its amount to 15 equivalents enhanced the yield of **3a** to 67% (Table S3, entry 8), indicating that the high concentration of substrate contributes to increasing the HAT event's probability of the triplet state chromone with substrate, reducing self-coupling of exciting state chromone. To further inhibit this self-coupling, we tried to increase the volume of the reaction solvent to decrease the concentration of the exciting state chromone. Preliminary screening of the reaction solvent volume (Table S4, entry 7) revealed that employing 6 ml of DCE delivered the target product **3a** in 73% yield (Table 1, entry 12). Variation of the irradiation

Table 1. Optimization of the reaction conditions. A mixture of **1a** (0.2 mmol) and **2a** in the solvent was irradiated with a 9-W light-emitting diode at room temperature under an argon atmosphere. Yields were determined by ^{1}H nuclear magnetic resonance spectroscopy using 1,4-dimethoxybenzene as an internal standard.



Entry	**2a**/mmol	Light	Solvent	Time/h	Yield%
1	2.0	365 nm	2 ml DCE	12	59
2	2.0	390 nm	2 ml DCE	12	29
3	2.0	405 nm	2 ml DCE	12	27
4	2.0	365 nm	2 ml MeCN	12	9
4	2.0	365 nm	2 ml EA	12	21
5	2.0	365 nm	2 ml DCM	12	54
6	2.4	365 nm	2 ml DCE	12	62
7	2.8	365 nm	2 ml DCE	12	65
8	3.0	365 nm	2 ml DCE	12	67
9	3.2	365 nm	2 ml DCE	12	66
10	3.6	365 nm	2 ml DCE	12	62
11	3.0	365 nm	4 ml DCE	12	68
12	3.0	365 nm	6 ml DCE	12	73 (66) [a]
13	3.0	365 nm	8 ml DCE	12	56
14	3.0	365 nm	6 ml DCE	10	64

[a]Isolated yield.

duration confirmed 12 h as the optimal reaction time (Table S5), ensuring sufficient photon absorption while avoiding decomposition due to overexposure. Subsequently, temperature was evaluated over the range of 0 to 40 °C (Table S6). The reaction exhibited the highest efficiency at room temperature, while lower temperatures likely reduced the efficiency of HAT, and higher temperatures may decrease the stability of the triplet chromone excited state. The effect of LED power (3 to 10 W) on the yield of **3a** was evaluated (Table S7), reaching a maximum at 9 W; the higher power slightly decreased the yield, likely due to side reactions. On the basis of these results, the standard reaction conditions for subsequent investigations were established as follows: chromone (**1a**, 0.2 mmol) and benzodioxole (**2a**, 3 mmol) in DCE (6 ml) under an argon atmosphere irradiated with a 9-W 365-nm LED light source for 12 h.

Scope of the reaction

Under the optimized conditions, we explored the substrate scope of ether derivatives (Fig. 2). Unsubstituted benzodioxole reacted smoothly to afford product **3a** in 66% yield, and its *S*-configuration was unambiguously confirmed by x-ray crystallographic analysis. The introduction of electron-donating groups or halogen substituents (**3b** to **3d**) resulted in diminished yields, whereas electron-withdrawing groups enhanced the reactivity, delivering **3e** to **3i** in fair to good yields. Sesamin was also compatible with the reaction system, affording **3j**. Notably, the substrate scope was successfully expanded to various aliphatic and cyclic ethers, including anisole, propyl ether, butyl ether, *tert*-butyl methyl ether, methylal, dimethoxyethane, ethyl acetate, tetrahydrofuran, and 1,4-dioxane, all of which exhibited excellent compatibility. When ethyl acetate as a solvent was added in bulk, the yield of **3q** improved markedly compared to equimolar conditions. It afforded only a trace product. Diastereomers **3r** to **3t** were readily separable by column chromatography. Substrates with multiple reactive sites reacted selectively at a single C–H bond. This process produced **3u** as the only product. Additionally, the reaction was applicable to simple alcohols upon the addition of boric acid to facilitate α-C–H bond activation [73,74] (Table S8), providing **3v** to **3x** in moderate yields.

To further broaden substrate diversity, we explored N-, P-, and S-containing compounds (Fig. 3), obtaining products **4a** to **4h** in moderate yields. Considering the higher C–H bond dissociation energies (BDEs) of cyclic alkanes, we evaluated the HAT capability of photoexcited triplet-state chromone with cyclopentane, cyclohexane, cycloheptane, and adamantane, leading to **4j** to **4l** in moderate yields. Toluene was also tolerated under standard conditions, affording **4m**. We then examined substituted chromones bearing modifications on the benzene ring, which furnished derivatives **5a** to **5h** in 41% to 67% yields. When chromones bear phenol, carboxylic acid, or nitro substituents on the benzene ring, corresponding target products were not observed. It is proposed that phenol and carboxylic acid groups may quench the HAT process via labile hydrogen atoms, while nitro substituents alter the electron density of the substrate, thereby affecting its excited state and reducing its ability to participate in the reaction.

To assess the practical synthetic utility of this protocol, a gram-scale reaction of **1a** (7 mmol) with **2a** (45 mmol) was performed in anhydrous DCE (80 ml) under argon. Irradiation at 365 nm for 12 h gave **3a** in 60% isolated yield after purification (Fig. 4). Further transformations of **3a** were carried out (Fig. 4). The carbonyl group of **3a** can be effectively converted into idenehydrazine (**A1**), aldehyde oxime (**B1**), and hydroxyl (**C1**) structures with excellent yields, and **3a** can be condensed with an aldehyde to yield the target compound **D1**. Single-crystal x-ray diffraction further verified that compounds **A1**, **B1**, and **D1** exhibit the E configuration.

Investigation and proposal of the reaction mechanism

To elucidate the intrinsic reaction mechanism, a systematic set of mechanistic investigations was performed. Time-correlated single photon counting (TCSPC) measurements showed that the fluorescence lifetime of the singlet excited state of chromone was 3.2 ns alone and 2.8 ns in the presence of benzodioxole. This indicates that the singlet state is not markedly quenched and suggests that substrate activation may proceed via the triplet excited state of chromone (Figs. S2 and S3). The addition of 1,1,4,4-tetramethylbutadiene, a selective triplet quencher, markedly suppressed the reaction, indicating the involvement of a triplet excited state [75] (Fig. 5A). The addition of 2,2,6,6-tetramethyl-1-piperidinyloxy (TEMPO) as a radical scavenger fully suppressed the formation of **3a**, and high-resolution mass spectrometer (HRMS) analysis confirmed the formation of TEMPO–radical adducts **K1** and **K2** (Fig. 5B), supporting a radical-based pathway. Kinetic isotope effect (KIE) studies using cyclohexane and cyclohexane-d_{12} in competitive and parallel experiments gave values of 1.82 and 1.22, respectively, indicating that the reaction rate is not governed by C(sp^3)–H bond cleavage (Fig. 5C). Intermittent irradiation (photo-switching) experiments demonstrated that product formation ceased in the dark and resumed upon re-illumination, confirming the necessity of continuous photoexcitation (Fig. 5D). In addition, the moderate quantum yield ($\Phi = 0.384$) suggests that an extended radical chain pathway is unlikely. Stern–Volmer fluorescence measurements show a slight concentration-dependent change in the excited-state emission intensity of chromone (**1a**) upon addition of cyclohexane (Fig. 5E), indicating that fast substrate-induced excited-state deactivation is not dominant. Furthermore, deuterium-labeling experiments using cyclohexane-d_{12} afforded product **4j**-d_{12} [25,76]. Given that the C–H bond at the 3-position of **4j**-d_{12} (BDE = 90 to 94 kcal/mol) [77] is weaker than that of cyclohexane (BDE =100 kcal/mol), deuterium incorporation is proposed to occur via HAT from an intermediate species **C**, consistent with BDE considerations [78] (Fig. 5F).

To provide more robust support for the proposed catalytic cycle, we conducted density functional theory (DFT) calculations encompassing all intermediates and transition states associated with the reaction of chromone (**1a**) and benzodioxole (**2a**) (Fig. 5G). Excitation of chromone at 365 nm generates the triplet state **A** (75.5 kcal/mol above the ground state). Hydrogen-atom transfer from **2a** to **A** proceeds through transition state **TS1** ($\Delta G^{\ddagger}$ = 9.7 kcal/mol) and furnishes radical pair **B**/**C**. **B** adds to a ground-state chromone in a Giese reaction via **TS2** ($\Delta G^{\ddagger}$ =13.3 kcal/mol) to deliver intermediate **D**. **D** then acquires a hydrogen atom by 1 of 2 routes: direct HAT from **2a** (**TS3**, $\Delta G^{\ddagger}$ =21.6 kcal/mol) or transfer from radical **C** (**TS4**, $\Delta G^{\ddagger}$ =-2.7 kcal/mol). The markedly lower barrier associated with **TS4** demonstrates that hydrogen transfer from **C** to **D** is both kinetically and thermodynamically favored (exergonic by 2.7 kcal/mol), giving rise to product **3a** along with the regeneration of chromone. These computational results are consistent

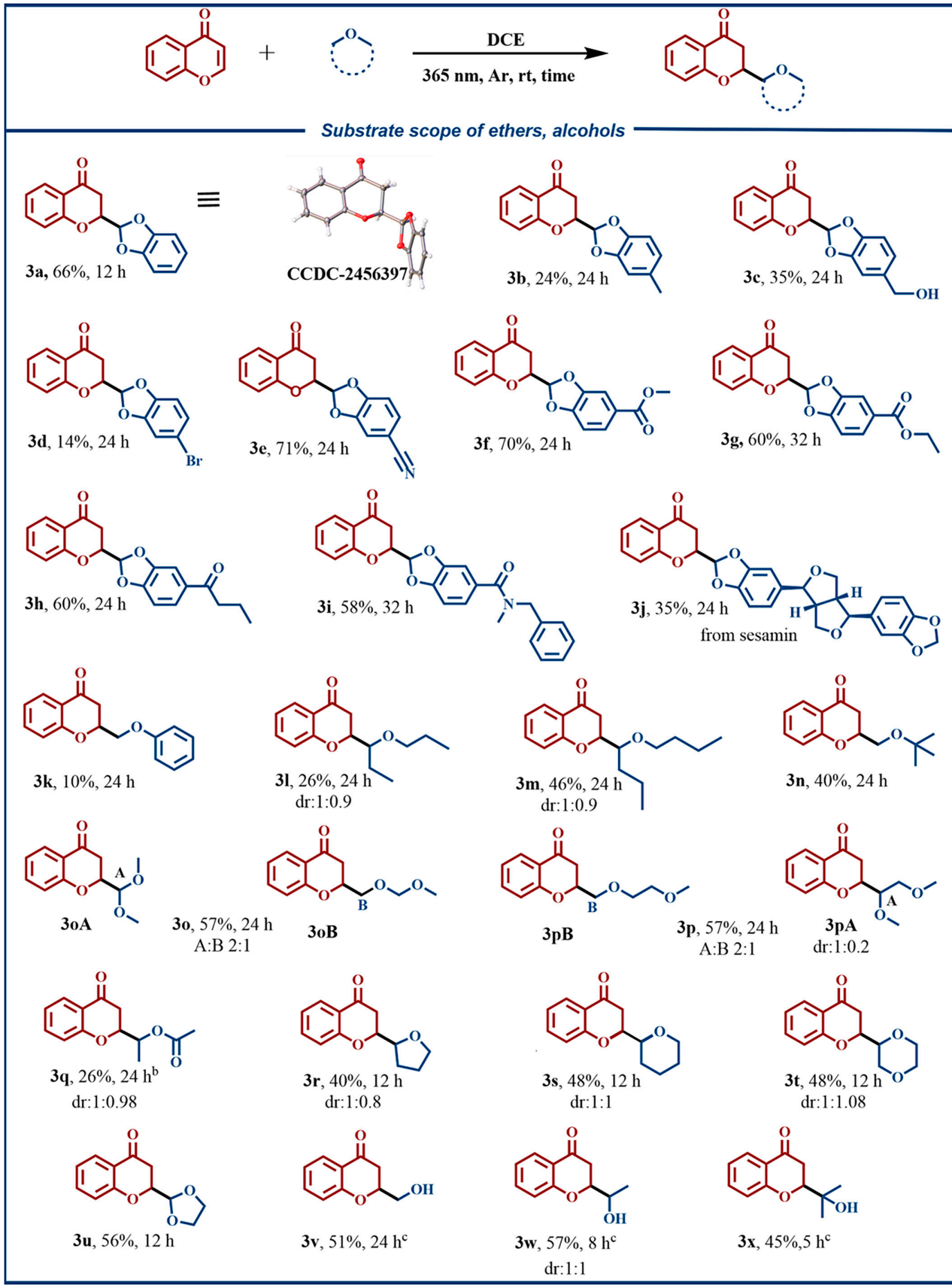


Fig. 2. Substrate scope. [a] Reaction conditions: A mixture of **1a** (0.2 mmol) and **2** (3 mmol) in DCE (6 ml) was irradiated with a 9-W light-emitting diode (LED) ($\lambda = 365$ nm) at room temperature under an argon atmosphere. Isolated yield and reaction times are indicated below each product. [b] **1a** (0.2 mmol) in ethyl acetate (2 ml). [c] **1a** (0.2 mmol) and $B(OH)_3$ (0.3 mmol) in the corresponding alcohol (2 ml).

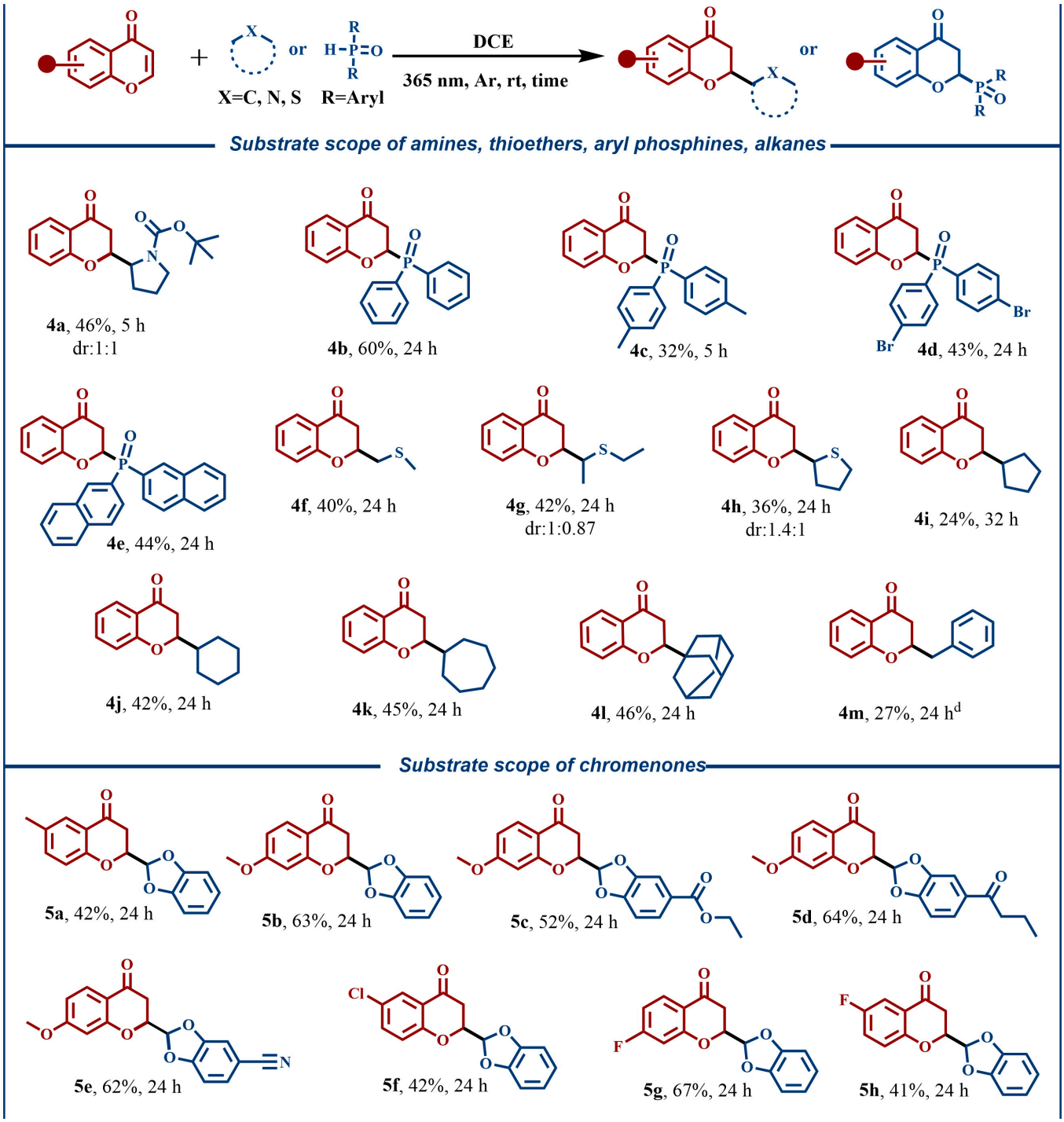


Fig. 3. Substrate scope. [a] Reaction conditions: A mixture of **1** (0.2 mmol) and **2** (3 mmol) in DCE (6 ml) was irradiated with a 9-W LED (λ = 365 nm) at room temperature under an argon atmosphere. Isolated yield and reaction times are indicated below each product. [d] **1a** (0.2 mmol) in toluene (2 ml).

with the deuterium-labeling experiments and strongly support the proposed mechanism.

Based on the results of mechanistic interrogations, a plausible reaction mechanism is proposed (Fig. 6). Under 365 nm irradiation, chromone (**1a**) undergoes photoexcitation and intersystem crossing to form the triplet diradical species **A**. A hydrogen atom is then transferred from **2a** to **A** through transition state **TS1**, with an activation energy of 9.7 kcal/mol, generating radicals **B** and **C**. Radical **B** subsequently reacts with a ground-state chromone molecule via **TS2** ($\Delta G^{\ddagger}$ = 13.3 kcal/mol) to form intermediate **D**. In the final step, **D** abstracts a hydrogen atom from radical **C**, producing the product **3a** and regenerating the chromone catalyst, thus completing the catalytic cycle.

The mechanism pinpoints a dual duty for photoexcited chromone: the molecule is simultaneously the substrate and the HAT agent. Earlier radical-addition protocols operate through thermal initiation or metal-mediated channels; in those setups,

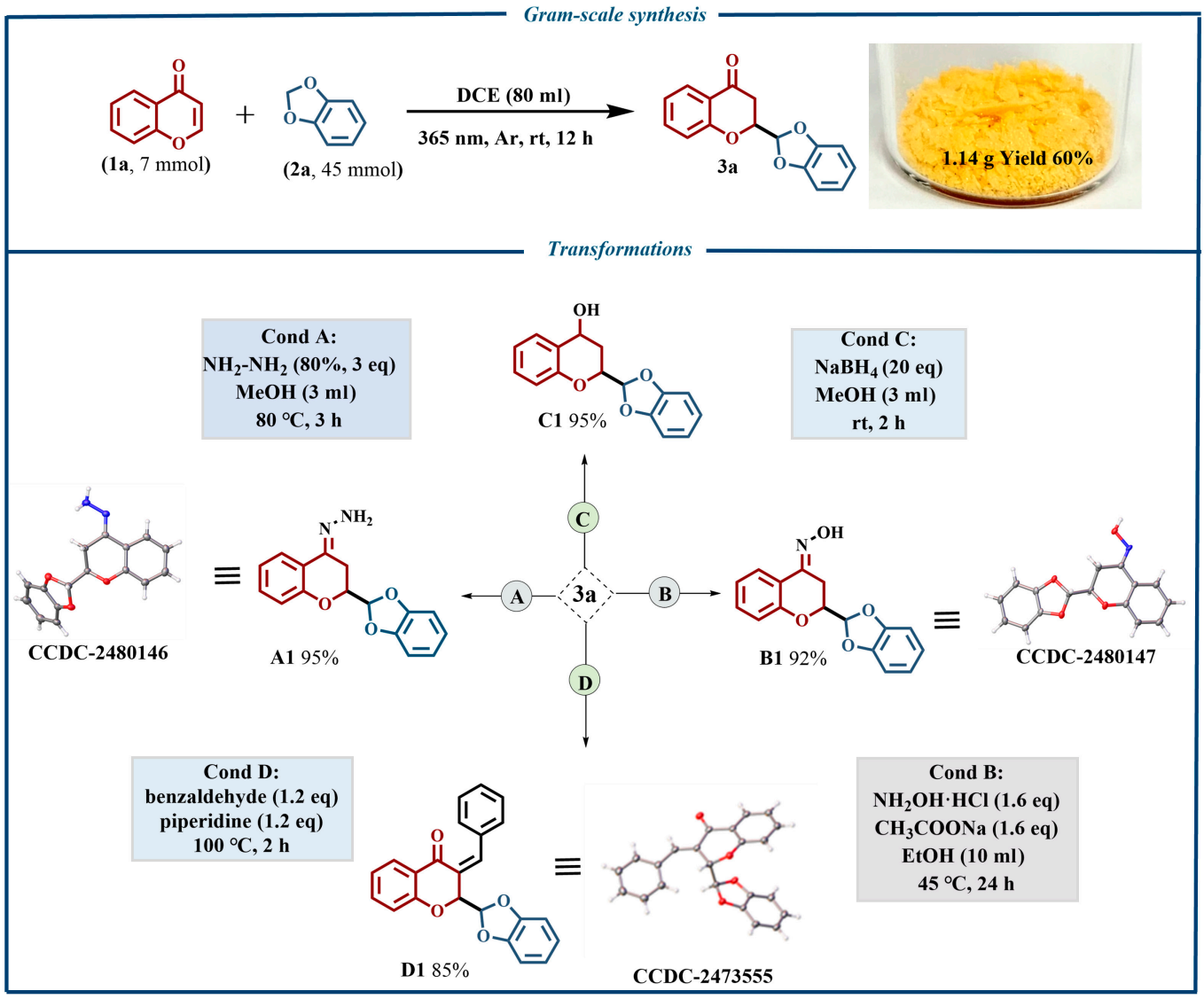


Fig. 4. Gram-scale synthesis and transformations.

radicals form exclusively to execute HAT and never engage the substrate directly. Our photocatalytic platform breaks with that tradition. It harnesses the excited-state chromone itself. This built-in reactivity opens normally unreactive C–H and P–H bonds under mild conditions, streamlines the operational sequence, and removes the usual requirements for metal catalysts or external radical initiators.

Conclusion

Herein, we report a photocatalytic Giese addition protocol wherein chromone derivatives serve dually as substrates and HAT mediators. This transformation occurs under mild conditions and does not require external photocatalysts, metal additives, stoichiometric oxidants, or additional HAT reagents, in line with green chemistry principles. This method is compatible with a wide variety of substrates, allowing efficient activation of inert C–H bonds in ethers, esters, alcohols, alkanes, amines, sulfides, and P–H bonds in arylphosphines. These 2-substituted 4-chromanones are valuable intermediates. They allow various post-synthetic modifications and illustrate the practicality of this strategy. Mechanistic investigations (comprising control experiments, spectroscopic analyses, and DFT calculations) collectively support a photoinduced, chromone-mediated HAT catalytic cycle. Overall, this work establishes an efficient, metal-free, and sustainable route to 2-substituted 4-chromanone derivatives through direct photocatalytic HAT activation.

Materials and Methods

All reagents and solvents of reagent grade were obtained from commercial suppliers and used as received without additional purification. Nuclear magnetic resonance spectra were recorded in $CDCl_3$ on JEOL JNM-ECZ600R/M1 (^{1}H 600 MHz, ^{13}C 15 MHz), JEOL-ECX-500 (^{1}H 500 MHz, ^{13}C 126 MHz, ^{19}F 471 MHz, ^{31}P 202 MHz), or Bruker AG-400 (^{1}H 400 MHz, ^{13}C 101 MHz) spectrometers. HRMS analyses were carried out on a Thermo Scientific Orbitrap with an ESI source. Thin-layer chromatography (TLC) was performed on 0.25-mm silica gel plates (Merck), and flash chromatography used 300 to 400 mesh silica gel with petroleum ether/ethyl acetate.

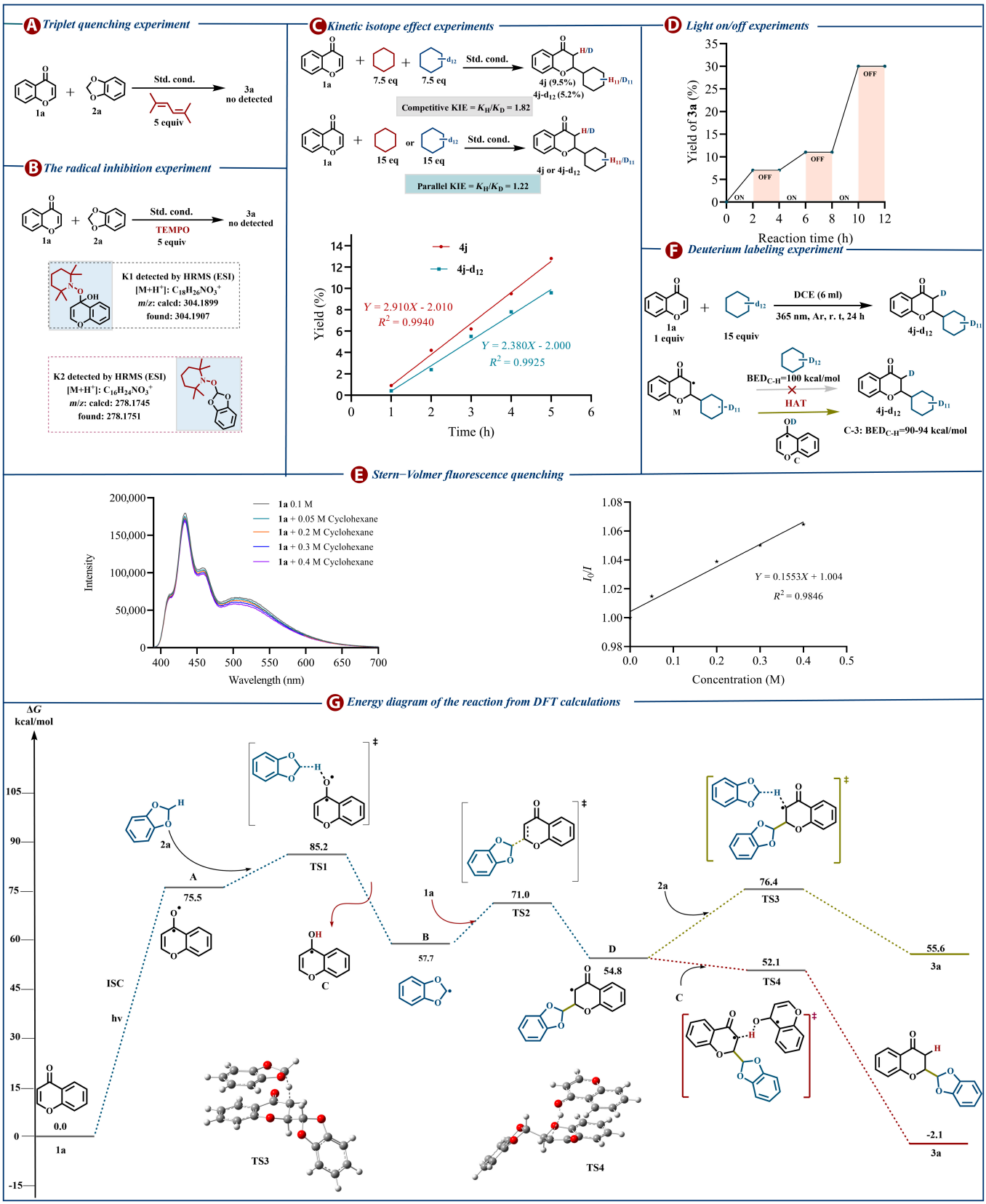


Fig. 5. (A) Triplet quenching experiment. (B) The radical inhibition experiment. (C) Kinetic isotope effect experiment. (D) Light on/off experiment. (E) Stern–Volmer fluorescence quenching. (F) Deuterium labeling experiment. (G) Energy diagram of the reaction from DFT calculations.

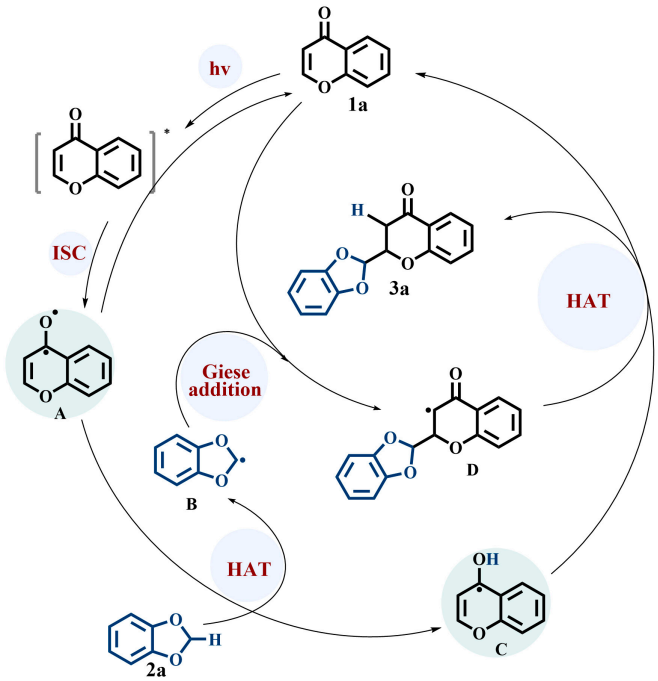


Fig. 6. Proposed reaction mechanism.

General procedure: Substrate **1** (0.2 mmol) and solid substrate **2** (3.0 mmol) were added in sequence to a 10-ml glass vial with a magnetic stir bar, which was then sealed. The vial was evacuated and refilled with argon 3 times using an oil pump. Anhydrous DCE (6.0 ml) was then added as the reaction solvent. For liquid substrates **2** (3.0 mmol) or alcohols (2.0 ml), the addition was performed after the completion of the argon purging process; stirring of the resulting mixture was performed under a 9-W, 365-nm LED light for 5 to 32 h. TLC was employed to track the reaction progress. Upon completion, the reaction mixture was concentrated under reduced pressure, and the target product was isolated via flash column chromatography (eluent: petroleum ether/ethyl acetate).

Acknowledgments

Funding: This work was supported by the National Natural Science Foundation of China (U23A20201, 32372610, 32160661, and 32202359), the National Key Research and Development Program of China (2022YFD1700300 and 2024YFE0214300), the Central Government Guides Local Science and Technology Development Fund Projects (Qiankehezhongyindi [2023] 001 and Qiankehezhongyindi [2024] 007), the Scientific and Technological Innovation Platform Research Project of Guizhou Province (CXPTXM [2025] 012), the Major Scientific and Technological Achievement Transformation Project of Guizhou Province (Qian Ke He Zhong Yin Di [2024] 027), the Outstanding Young Scientific and Technological Talent Project of Guizhou Province (Qian Ke He Ping Tai Ren Cai YQK [2023] 004), and the Bijie Tobacco Project (No. 2024SMXM02).
Author contributions: Y.X. conceived the study, conducted the investigation, and wrote the original draft. J.Z. curated data and contributed to manuscript revision. W.J. assisted with data curation and manuscript editing. Y.Z. participated in data organization and manuscript revision. W.M.W.W.K. contributed to data management and manuscript editing. X.Z. supervised the project, validated the results, revised the manuscript, and acquired funding. S.Y. supervised the research, validated the findings, revised the manuscript, and secured funding.
Competing interests: The authors declare that they have no competing interests.

Data Availability

All experimental data are available in the Supplementary Materials or from the corresponding authors upon request. The x-ray crystallographic coordinates for structures reported in this article have been deposited at the Cambridge Crystallographic Data Centre (CCDC), under deposition numbers CCDC 2456397 (3a), 2480146 (A1), 2480147 (B1), and 2473555 (D1). The data can be obtained free of charge from The Cambridge Crystallographic Data Centre via http://www.ccdc.cam.ac.uk/data_request/cif

Supplementary Materials

Graphical Abstract
Supplementary Text
Tables S1 to S14
Schemes S1 to S10
Figs. S1 to S191

References

1. Gu G, Zhang T, Zhao J, Zhao W, Tang Y, Wang L, Cen S, Yu L, Zhang D. New dimeric chromanone derivatives from the mutant strains of *Penicillium oxalicum* and their bioactivities. *RSC Adv*. 2022;12:22377–22384.
2. Yang PS, Dai JM, Gu XJ, Xiong W, Huang DQ, Qiu SY, Zheng JN, Li Y, Yang FX, Zhou M. Indole alkaloids and chromones from the stem bark of *Cassia alata* and their antiviral activities. *Molecules*. 2022;27(10):3129.
3. Valdomir G, Tietze LF. Chromanone lactones: A neglected group of natural products—Isolation, structure elucidation, bioactivity, and synthesis. *Eur J Org Chem*. 2022;2022(20):Article e202200201.
4. Gaspar A, Garrido EMPJ, Borges F, Garrido JMPJ. Biological and medicinal properties of natural chromones and chromanones. *ACS Omega*. 2024;9(20):21706–21726.
5. Feng L, Maddox MM, Alam MZ, Tsutsumi LS, Narula G, Bruhn DF, Wu X, Sandhaus S, Lee RB, Simmons CJ, et al. Synthesis, structure–activity relationship studies, and antibacterial evaluation of 4-chromanones and chalcones, as well as olympicin A and derivatives. *J Med Chem*. 2014;57(20):8398–8420.
6. Liu S-S, Zeng D, Zhang T-H, Hu J-H, Yang B-X, Yang J, Zhou X, Wang P-Y, Liu L-W, Wu Z-B, et al. Novel spiro[chromanone-2,4′-piperidine]-4-one derivatives as potential inhibitors of fatty acid synthesis in pathogens: Design, synthesis, and biological evaluation. *Eur J Med Chem*. 2023;250:Article 115215.
7. Fischer W, Currais A, Liang Z, Pinto A, Maher P. Old age-associated phenotypic screening for Alzheimer's disease drug candidates identifies sterubin as a potent neuroprotective compound from Yerba santa. *Redox Biol*. 2019;21:Article 101089.
8. Shen YC, Wang L-T, Khalil AT, Kuo Y-H. Chromanones and dihydrocoumarins from *Calophyllum blancoi*. *Chem Pharm Bull*. 2004;52:402–405.

9. Seifert T, Malo M, Kokkola T, Engen K, Fridén-Saxin M, Wallén EAA, Lahtela-Kakkonen M, Jarho EM, Luthman K. Chroman-4-one- and chromone-based sirtuin 2 inhibitors with antiproliferative properties in cancer cells. *J Med Chem*. 2014;57(23):9870–9888.
10. Zhao J, Fang H, Qian P, Han J, Pan Y. Metal-free oxidative C(sp^3)–H bond functionalization of alkanes and conjugate addition to chromones. *Org Lett*. 2014;16(20):5342–5345.
11. Yu J-T, Li Y, Chen R, Yang Z, Pan C. DTBP-promoted site-selective α-alkoxyl C–H functionalization of alkyl esters: Synthesis of 2-alkyl ester substituted chromanones. *Org Biomol Chem*. 2021;19:4520–4528.
12. Chen R, Yu J-T, Cheng J. Metal-free oxidative decarbonylative alkylation of chromones using aliphatic aldehydes. *Org Biomol Chem*. 2018;16:3568–3571.
13. Chen R, Yu J-T, Cheng J. Site-specific hydroxyalkylation of chromones *via* alcohol mediated minisci-type radical conjugate addition. *Org Biomol Chem*. 2018;16(11):1823–1827.
14. Zimmerman JR, Manpadi M, Spatney R. Tin-free radical reactions under minimal solvent conditions for the synthesis of substituted chromones and coumarins. *Green Chem*. 2011;13:3103–3106.
15. Li S, Zhang L, He Q, Zhang X, Yang C. Synthesis of 2-alkyl-chroman-4-ones via cascade alkylation–dechlorination of 3-chlorochromones. *Org Biomol Chem*. 2021;19(24):5348–5352.
16. Wang J-Y, Chen X-L, Dong Y, Tang L, Zhang X-M. A synthetic strategy for 2-alkylchromanones: Fe(III)-catalyzed reductive cross-coupling of unactivated alkenes with chromones. *Synlett*. 2018;29(14):1851–1856.
17. Zhang LX, Qi MY, Tang ZR, Xu YJ. Heterostructure-engineered semiconductor quantum dots toward photocatalyzed-redox cooperative coupling reaction. *Research*. 2023;6:0073.
18. Lei B, Zhou G, Gong Z, Liu C, Zhou Y, Guro VP, Sun Y, Sheng J, Dong F. Dynamically cyclic Fe^{2+}/Fe^{3+} active sites as electron and proton-feeding centers boosting CO_2 photoreduction powered by benzyl alcohol oxidation. *Research*. 2025;8:0567.
19. Reischauer S, Pieber B. Emerging concepts in photocatalytic organic synthesis. *Science*. 2021;24(3):Article 102209.
20. Li QZ, He MH, Wang PT, Xiang DY, Hong LH, Zeng R, Li JL. Alkene diversification through a molecular recasting strategy enabled by N-heterocyclic carbene and photoredox dual catalysis. *Research*. 2025;8:1010.
21. Xie J, Hou J, Bao C, Jin M. Visible-light-catalyzed cascade radical cyclization for 3-substituted chroman-4-ones. *J Org Chem*. 2025;90(47):16771–16778.
22. Han S, Liu L, Meng J, Li M, Cao Q, Shen Z. Photoredox iron-catalyzed decarboxylative radical cyclization for the synthesis of oxindoles and chroman-4-ones. *J Org Chem*. 2025;90(21):7062–7069.
23. Mei YT, Guo ZY, Liu FQ, Wang SS, Yang D, Jing LH, Shi MS. Organophotocatalytic acyltrifluoromethylation of unactivated alkenes enabled the efficient synthesis of CF_3-substituted chroman-4-ones. *Chem Commun*. 2025;61(64):11959–11962.
24. Lei Z, Zhang W, Wu J. Photocatalytic hydrogen atom transfer-induced Arbuzov-type α-C(sp^3)–H phosphonylation of aliphatic amines. *ACS Catal*. 2023;13:16105–16113.
25. Sarkar S, Wagulde S, Jia X, Gevorgyan V. General and selective metal-free radical α-C–H borylation of aliphatic amines. *Chem*. 2022;8(11):3096–3108.
26. Cao H, Kuang Y, Shi X, Wong KL, Tan BB, Kwan JMC, Liu X, Wu J. Photoinduced site-selective alkenylation of alkanes and aldehydes with aryl alkenes. *Nat Commun*. 2020;11:1956.
27. Golden DL, Suh S-E, Stahl SS. Radical C(sp^3)–H functionalization and cross-coupling reactions. *Nat Rev Chem*. 2022;6:405–427.
28. Capaldo L, Ravelli D, Fagnoni M. Direct photocatalyzed hydrogen atom transfer (HAT) for aliphatic C–H bonds elaboration. *Chem Rev*. 2021;122(2):1875–1924.
29. Cao H, Tang X, Tang H, Yuan Y, Wu J. Photoinduced intermolecular hydrogen atom transfer reactions in organic synthesis. *Chem Catalysis*. 2021;1(3):523–598.
30. Perry IB, Brewer TF, Sarver PJ, Schultz DM, DiRocco DA, MacMillan DWC. Direct arylation of strong aliphatic C–H bonds. *Nature*. 2018;560:70–75.
31. Shen Y, Gu Y, Martin R. sp^3 C–H arylation and alkylation enabled by the synergy of triplet excited ketones and nickel catalysts. *J Am Chem Soc*. 2018;140(38):12200–12209.
32. Cheng X, Lu H, Lu Z. Enantioselective benzylic C–H arylation via photoredox and nickel dual catalysis. *Nat Commun*. 2019;10:3549.
33. Le C, Liang Y, Evans RW, Li X, MacMillan DWC. Selective sp^3 C–H alkylation via polarity-match-based cross-coupling. *Nature*. 2017;547:79–83.
34. Si X, Zhang L, Hashmi ASK. Benzaldehyde- and nickel-catalyzed photoredox C(sp^3)–H alkylation/arylation with amides and thioethers. *Org Lett*. 2019;21(16):6329–6332.
35. Ackerman LKG, Martinez Alvarado JI, Doyle AG. Direct C–C bond formation from alkanes using Ni-photoredox catalysis. *J Am Chem Soc*. 2018;140(43):14059–14063.
36. Monirialamdari M, Albrecht A. Decarboxylative photoinduced ligand-to-metal charge transfer reaction: Synthesis of 2-substituted chroman-4-ones. *Chem Commun*. 2024;60(10):1265–1268.
37. Moczulski M, Kowalska E, Kuśmierek E, Albrecht Ł, Albrecht A. Visible-light synthesis of 4-substituted-chroman-2-ones and 2-substituted-chroman-4-ones via doubly decarboxylative Giese reaction. *RSC Adv*. 2021;11:27782–27786.
38. Entgelmeier LM, Mori S, Sendo S, Yamaguchi R, Suzuki R, Yanai T, García Mancheño O, Ohmatsu K, Ooi T. Zwitterionic acridinium amidate: A nitrogen-centered radical catalyst for photoinduced direct hydrogen atom transfer. *Angew Chem Int Ed Engl*. 2024;(43):63, Article e202404890.
39. Qiao L, Yang W, Zhao X, Li E, Chen X, Qu L, Yu B. Decatungstate-photocatalyzed radical addition of C(sp^3)–H to azauracils. *Org Chem Front*. 2024;11:5791–5797.
40. Fan X-Z, Rong J-W, Wu H-L, Zhou Q, Deng H-P, Tan J-D, Xue C-W, Wu L-Z, Tao H-R, Wu J. EosinY as a direct hydrogen-atom transfer photocatalyst for the functionalization of C−H bonds. *Angew Chem Int Ed Engl*. 2018;57:8514–8518.
41. Yan J, Tang H, Kuek EJR, Shi X, Liu C, Zhang M, Piper JL, Duan S, Wu J. Divergent functionalization of aldehydes photocatalyzed by neutral eosin Y with sulfone reagents. *Nat Commun*. 2021;12:7214.
42. Treacy SM, Rovis T. Copper catalyzed C(sp^3)–H bond alkylation via photoinduced ligand-to-metal charge transfer. *J Am Chem Soc*. 2021;143(7):2729–2735.
43. Miao W, Huang Y, Hu P. Terminal C (sp^3)–H borylation through intermolecular radical sampling. *Science*. 2024;383(6682):537–544.
44. Li H-C, Zhang M, Lv Q, Sun K, Chen X-L, Qu L, Yu B. Homogeneous catalysis and heterogeneous separation: Ionic liquids as recyclable photocatalysts for hydroacylation of olefins. *Chin Chem Lett*. 2025;36(2):Article 110579.
45. Cuthbertson JD, MacMillan DWC. The direct arylation of allylic sp^3 C–H bonds via organic and photoredox catalysis. *Nature*. 2015;519:74–77.

46. Panferova LI, Zubkov MO, Kokorekin VA, Levin VV, Dilman AD. Using the thiyl radical for aliphatic hydrogen-atom transfer: Thiolation of unactivated C−H bonds. *Angew Chem Int Ed Engl*. 2021;60(6):2849–2854.
47. Wang W, Yan S-S, Liu Y, Zhu J-S, Yang J-W, Xu J-C, Tao Y-Y, Li J-C, Song L, Ye J-H, et al. Photocatalytic 1,2-dicarboxylation of unactivated alkynes with CO_2. *J Am Chem Soc*. 2025;147(27):23715–23723.
48. Jeffrey JL, Terrett JA, MacMillan DWC. O–H hydrogen bonding promotes H-atom transfer from α C–H bonds for C-alkylation of alcohols. *Science*. 2015;349(6255):1532–1536.
49. Hu H, Shi Z, Guo X, Zhang F-H, Wang Z. A radical approach for asymmetric α-C–H addition of *N*-sulfonyl benzylamines to aldehydes. *J Am Chem Soc*. 2024;146(8):5316–5323.
50. Mandigma MJP, Kaur J, Barham JP. Organophotocatalytic mechanisms: Simplicity or naïvety diverting reactive pathways by modifications of catalyst structure, redox states and substrate preassemblies. *ChemCatChem*. 2023;15(11): Article e202201542.
51. Wu M, Wu Z, Ang HT, Wang B, Liu T, Wu S, Lei Z, Liaw MW, Chanmungkalakul S, Lee C-LK, et al. Enhanced reactivity of acridinium perchlorate: Harnessing redox mediators for trace chloride activation in hydrogen atom transfer photocatalysis. *ACS Catal*. 2024;14:9364–9373.
52. Waele VD, Poizat O, Fagnoni M, Bagno A, Ravelli D. Unraveling the key features of the reactive state of decatungstate anion in hydrogen atom transfer (HAT) photocatalysis. *ACS Catal*. 2016;6:7174–7182.
53. Tu J-L, Zhu Y, Li P, Huang B. Visible-light induced direct C(sp^3)–H functionalization: Recent advances and future prospects. *Org Chem Front*. 2024;11(18):5278–5305.
54. Majek M, Filace F, von Wangelin AJ. On the mechanism of photocatalytic reactions with eosin Y. *Beilstein J Org Chem*. 2014;10:981–989.
55. Bosveli A, Montagnon T, Kalaitzakis D, Vassilikogiannakis G. Eosin: A versatile organic dye whose synthetic uses keep expanding. *Org Biomol Chem*. 2021;19(15):3303–3317.
56. Gevorgyan V, Iziumchenko V. Recent advances in dual triplet ketone/transition-metal catalysis. *Synlett*. 2023;34(12): 1289–1308.
57. Capaldo L, Quadri LL, Ravelli D. Photocatalytic hydrogen atom transfer: The philosopher's stone for late-stage functionalization? *Green Chem*. 2020;22:3376–3396.
58. Norrish RGW, Bamford CH. Photo-decomposition of aldehydes and ketones. *Nature*. 1937;140:195–196.
59. Zeng H, Yin R, Zhao Y, Ma J-A, Wu J. Modular alkene synthesis from carboxylic acids, alcohols and alkanes via integrated photocatalysis. *Nat Chem*. 2024;16(11):1822–1830.
60. Liu BY, Zhang ZC, Song ZL, Yuan HY, Li YH, Zhang ZC, Yang Z. Formation of multiple naturally occurring meroterpenoid scaffolds by the Norrish-Yang reaction of a p-benzoquinone. *Angew Chem Int Ed Engl*. 2024;64(3): Article e202415249.
61. Zhan T, Yang L, Chen Q, Weng R, Liu X, Feng X. Chiral Lewis acid-catalyzed Norrish type II cyclization to synthesize α-oxazolidinones via enantioselective protonation. *CCS Chem*. 2023;5:2101–2110.
62. Dantas JA, Correia JTM, Paixão MW, Corrêa AG. Photochemistry of carbonyl compounds: Application in metal-free reactions. *ChemPhotoChem*. 2019;3(7):506–520.
63. Matsumoto K, Nakajima M, Nemoto T. Visible light-induced direct $S_0 \rightarrow T_n$ transition of benzophenone promotes C(sp^3)–H alkynylation of ethers and amides. *J Org Chem*. 2020;85(18):11802–11811.
64. Dewanji A, Krach PE, Rueping M. The dual role of benzophenone in visible-light/nickel photoredox-catalyzed C−H arylations: Hydrogen-atom transfer and energy transfer. *Angew Chem Int Ed Engl*. 2019;58(11):3566–3570.
65. von Zuben TW, Cariello Silva G, Salles AG. Visible light-driven metal-free synthesis of highly substituted pyrroles through C–H functionalisation. *Green Chem* 2021;23(11):6361–6365.
66. Zhang S, Cao S, Lin YM, Sha L, Lu C, Gong L. Photocatalyzed site-selective C(sp^3)–H sulfonylation of toluene derivatives and cycloalkanes with inorganic sulfinates. *Chinese J Catal*. 2022;43(3):564–570.
67. Ishida N, Masuda Y, Imamura Y, Yamazaki K, Murakami M. Carboxylation of benzylic and aliphatic C–H bonds with CO_2 induced by light/ketone/nickel. *J Am Chem Soc*. 2019;141(50):19611–19615.
68. Masuda Y, Ishida N, Murakami M. Aryl ketones as single-electron-transfer photoredox catalysts in the nickel-catalyzed homocoupling of aryl halides. *Eur J Org Chem*. 2016;2016(35):5822–5825.
69. Paul S, Guin J. Radical C(sp^3)–H alkenylation, alkynylation and allylation of ethers and amides enabled by photocatalysis. *Green Chem*. 2017;19(11):2530–2534.
70. Yan Y, Li G, Ma J, Wang C, Xiao J, Xue D. Photoinduced generation of ketyl radicals and application in C–C coupling withoutexternal photocatalyst. *Green Chem*. 2023;25:4129–4136.
71. Han T, Zhang S, Li J, Mou Q, Gao J, Cao B, Li C-J, Liu M. Direct metal-free homo-/cross-coupling of carbonyls with alcohols or imines under ambient light. *Green Chem*. 2025;27(25):7600–7607.
72. Pavlovich VS. Solvent polarity effect on excited-state lifetime of carotenoids and some dyes. *Biopolymers*. 2006;82(4):435–441.
73. Sun T, Jin R, Yang Y, Jia Y, Hu S, Jin Y, Wang Q, Li Z, Zhang Y, Wu J, et al. Direct α-C–H alkylation of structurally diverse alcohols via combined tavaborole and photoredox catalysis. *Org Lett*. 2022;24(41):7637–7642.
74. Merkens K, Sanosa N, Funes-Ardoiz I, Gómez-Suárez A. Accessing α-amino ketyl radicals from β-amino alcohols via chemoselective hydrogen atom transfer catalysis. *ACS Catal*. 2022;12(21):13186–13192.
75. Luo Y-X, Huang J, Wu G, Tang X-Y, Qu J-P. Visible-light-mediated deoxygenative transformation of 1,2-dicarbonyl compounds through energy transfer process. *Nat Commun*. 2024;15(1):9240.
76. Qin Y, Zhu L, Luo S. Organocatalysis in inert C–H bond functionalization. *Chem Rev*. 2017;117(13):9433–9520.
77. Hudzik JM, Bozzelli JW. Thermochemistry and bond dissociation energies of ketones. *J Phys Chem*. 2012;116(23):5707–5722.
78. Chen J, Lian Q, Jiang X, Zhang J, Luo X, Fang J, Wei W. Photocatalytic α-aminoalkyl radical addition of amines mediated by benzophenone under visible light. *Green Chem*. 2024;26(9):5471–5476.